

higher T_c 's, and as a further test of our hypotheses (vide supra), we have synthesized β -(ET) $_2$ AuI $_2$. This is the first linear-symmetric (I-Au-I) $^-$ triatomic metal-containing anion in an (ET) $_2$ X derivative, and one which has an anion length (~ 9.40 Å) intermediate between that of I $_3^-$ and IBr $_2^-$. This new salt has an ambient-pressure superconducting transition temperature almost double (~ 5 K) that of β -(ET) $_2$ IBr $_2$ and is the highest reported to date (vide infra).

Synthesis. Lustrous black crystals of β -(ET) $_2$ AuI $_2$ were grown by electrocrystallization (anhydrous and light-free conditions) by use of 9.3 mg of ET (Strem Chemical Co., 1.6 mM) as organic donor and 157 mg of *n*-Bu $_4$ NAuI $_2$ (15.1 mM) as supporting electrolyte at 23 °C in a standard H-cell. The anion and the supporting electrolyte were prepared by following a literature procedure.¹⁸ Its purity was confirmed by its melting point (78–79 °C) and elemental analysis. Anal. Calcd (found)¹⁹ for *n*-Bu $_4$ NAuI $_2$: C, 27.72 (27.68); H, 5.23 (5.32); N, 2.02(1.96); I, 36.61 (36.83). Dry THF was used as solvent, and a 1.0 μ A/cm 2 current density was applied. Crystal formation was observed within 24 h, and the fully grown distorted hexagons were harvested after about 1 week. The β -(ET) $_2$ X crystals are characterized by their room-temperature ESR line width of ~ 20 G.²⁰

Single-crystal X-ray analysis²¹ revealed that β -(ET) $_2$ AuI $_2$ is clearly isostructural (space group $P\bar{1}$, $V_c = 845.2$ (3) Å 3 , $Z = 1$) with β -(ET) $_2$ X, X = I $_3^-$ and IBr $_2^-$. The unit cell volumes for β -(ET) $_2$ X, X = I $_3^-$ and IBr $_2^-$, are 855.9 (2) and 828.7 (3) Å 3 , respectively, which indicates that, as expected, the (I-Au-I) $^-$ anion is of length intermediate between those of the two trihalide anions. The structure consists of discrete layers of AuI $_2^-$ anions between which is sandwiched a "corrugated sheet network"⁹ of ET molecules with short ($d_{S...S} \leq 3.60$ Å, the van der Waals radius sum for S) interstack S...S interactions. The loosely packed stacking of the ET entities is characterized by intrastack S...S distances exceeding 3.60 Å.

Superconductivity. The occurrence of a superconducting state in β -(ET) $_2$ AuI $_2$ was detected by rf penetration depth measurements at ambient pressure and at various applied magnetic fields, similar to measurements previously reported for the I $_3^-$ and IBr $_2^-$ derivatives.^{5,6,10} Figure 1 shows the change in resonant frequency as a function of temperature at zero applied magnetic field for a sample consisting of three relatively large single crystals. This sample gave an apparent onset temperature for bulk superconductivity (T_c) of 4.97 ± 0.06 K, which is the highest T_c yet observed at ambient pressure for an organic superconductor. Like the inductive superconducting transition curves for the trihalide derivatives, this figure shows a broad transition below T_c . Measurements of the onset temperatures of the individual crystals gave $T_c = 3.93 \pm 0.04$, 4.36 ± 0.04 , and 4.98 ± 0.08 K, respectively. Thus, the crystals of β -(ET) $_2$ AuI $_2$ have a range of T_c values like the trihalide derivatives but have a much larger spread in the extremes (~ 1 K in these experiments). Preliminary pressure studies using low-frequency ESR techniques described earlier⁷ indicate superconductivity is strongly depressed with pressure at a rate of 1 K/kbar.

Acknowledgment. Work at Argonne National Laboratory and Sandia National Laboratory is sponsored by the U.S. Department of Energy (DOE), Office of Basic Energy Sciences, Division of Materials Sciences, under Contracts W-31-109-Eng-38 and KC020202, respectively. We wish to thank D. L. Overmyer for his expert technical assistance.

Supplementary Material Available: Tables of crystal structure data collection and refinement parameters (Table X1) and final atom positional and anisotropic temperature factors (Table X2) (2 pages). Ordering information is given on any current masthead page.

(22) M.A.F., K.S.W., and L.N. are student research participants sponsored by the Argonne Division of Educational Programs from Indiana University of Pennsylvania, Indiana, PA, St. Michael's College, Winooski, VT, and DePaul University, Chicago, IL.

Chemistry and Materials Science and
Technology Divisions
Argonne National Laboratory
Argonne, Illinois 60439

Hau H. Wang
Mark A. Beno
Urs Geiser
Millicent A. Firestone²²
Kevin S. Webb²²
L. Nuñez²²
G. W. Crabtree
K. Douglas Carlson
Jack M. Williams*

Sandia National Laboratory
Albuquerque, New Mexico 87175

L. J. Azevedo
J. F. Kwak
J. E. Schirber

Received April 24, 1985

Transformation of Monoclinic CfBr $_3$ to Orthorhombic CfBr $_3$ by the Application of Pressure

Sir:

It has been shown previously that the orthorhombic form of anhydrous CfBr $_3$ can be synthesized by preparing $^{249}\text{BkBr}_3$ in its orthorhombic form and waiting for the ^{249}Bk ($t_{1/2} = 325$ d) to transmute to ^{249}Cf ($t_{1/2} = 351$ y) by β decay.¹ Both absorption spectrophotometric and X-ray powder diffraction analysis confirmed that, within the limits of sensitivity of these analytical techniques, the product of this transmutation is orthorhombic (PuBr $_3$ -type structure) CfBr $_3$. Up to now this has been the only way known to prepare the orthorhombic modification of CfBr $_3$. Two other structural forms are known for CfBr $_3$: AlCl $_3$ -type monoclinic and FeCl $_3$ -type rhombohedral.² We report here a new synthetic route to the orthorhombic form of CfBr $_3$. The advantage of this route, which requires the application of pressure, is that it is an active rather than passive one, thus giving control over the process to the experimenter.

A few micrograms of monoclinic CfBr $_3$ was loaded into a triangular-shaped diamond anvil pressure cell similar to that reported by Merrill and Bassett.³ A detailed description of the pressure cell and its use for spectral studies of actinide materials under pressure in conjunction with our microscope spectrophotometer⁴ will be published separately. The CfBr $_3$ was handled in a helium-atmosphere glovebox and was placed, along with silicone oil and ruby chips, in the 0.2 mm diameter hole of an Inconel gasket mounted on one of the diamond anvils. The oil

(18) Braunstein, P.; Clark, R. J. H.; Ramsay, W.; Forster, R.; Ingold, C. J. *Chem. Soc., Dalton Trans.* 1973, 1845.

(19) Analyses were performed by Midwest Microlab, Indianapolis, IN.

(20) Leung, P. C. W.; Beno, M. A.; Emge, T. J.; Wang, H. H.; Bowman, M. K.; Firestone, M. A.; Sowa, L. M.; Williams, J. M. *Mol. Cryst. Liq. Cryst.* 1985, 125, 113.

(21) X-ray data were collected on a Syntex P2 $_1$ diffractometer, and the triclinic unit cell data (space group $P\bar{1}$, $Z = 1$) are as follows (298 K): $a = 6.603$ (1) Å, $b = 9.015$ (2) Å, $c = 15.403$ (4) Å, $\alpha = 94.95$ (2)°, $\beta = 96.19$ (2)°, $\gamma = 110.66$ (1)°, $V = 845.2$ (3) Å 3 , $\rho_{\text{obsd}} = 2.39$ (8) g/cm 3 , and $\rho_{\text{calcd}} = 2.40$ g/cm 3 . Diffraction data (ω scan, Mo K α radiation, graphite monochromator, $\lambda = 0.7107$ Å) were collected at 298 K in the range $4^\circ < 2\theta < 50^\circ$, and 3406 data were averaged ($R_{\text{int}}(F) = 1.6\%$) to yield 2969 independent reflections, which were corrected for absorption ($\mu = 71.15$ cm $^{-1}$), with $T_{\text{min}} = 0.136$ and $T_{\text{max}} = 0.588$. Full-matrix least-squares refinement (all atoms except hydrogen were refined with anisotropic temperature factors, 178 parameters) yielded $R(F) = 4.3\%$ and $R_w(F) = 3.4\%$ (GOF = 1.85). The crystal structure is fully ordered, and the (I-Au-I) $^-$ anion Au-I bond distance is 2.5610 (6) Å.

(1) Young, J. P.; Haire, R. G.; Peterson, J. R.; Ensor, D. D.; Fellows, R. L. *Inorg. Chem.* 1980, 19, 2209.

(2) Burns, J. H.; Peterson, J. R.; Stevenson, J. N. *J. Inorg. Nucl. Chem.* 1975, 37, 743.

(3) Merrill, L.; Bassett, W. A. *Rev. Sci. Instrum.* 1974, 45, 290.

(4) Young, J. P.; Haire, R. G.; Fellows, R. L.; Peterson, J. R. *J. Radioanal. Chem.* 1978, 43, 479.

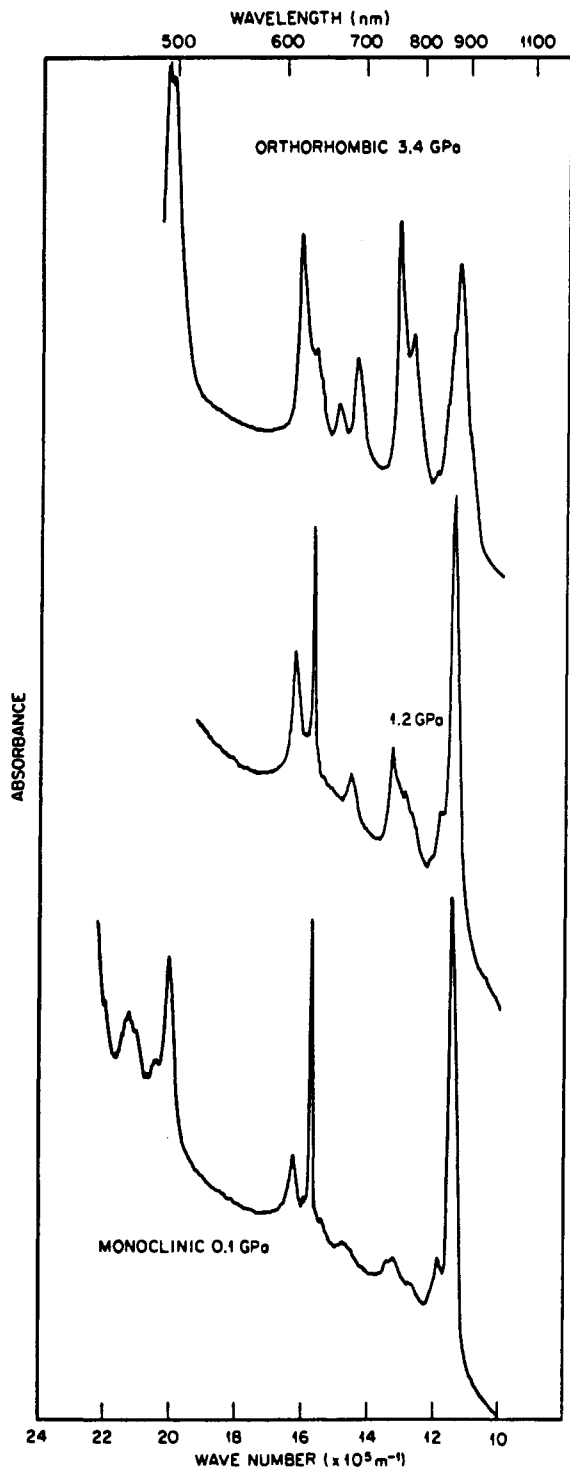


Figure 1. Room-temperature absorption spectra of $^{249}\text{CfBr}_3$ in two crystallographic forms (AlCl_3 -type monoclinic, PuBr_3 -type orthorhombic) at various pressures.

served as the pressure-transmitting medium, while the ruby allowed determination of the applied pressure by means of the ruby fluorescence technique using the nonlinear scale.⁵ The ruby was excited by the 514.5-nm radiation of an argon ion laser, and its fluorescent line near 694.2 nm was measured in a back-scattering mode with a Raman microprobe attached to a Ramanor HG-2S spectrometer. Spectrophotometric analysis of the CfBr_3 in the sealed pressure cell was carried out at room temperature in air. Pressure on the CfBr_3 sample was increased in steps by tightening screws at the corners of the triangular cell. The absorption

spectrum of the CfBr_3 sample and the fluorescent emission of ruby were obtained at each step. Assignment of the crystal structure exhibited by the CfBr_3 sample in this work was based on matching its absorption spectrum with those obtained from previous CfBr_3 samples that were sealed in silica capillaries and subjected to analysis by both absorption spectrophotometry and X-ray powder diffraction.¹

Three of the absorption spectra obtained in the present work are shown in Figure 1. The spectral features stem from Laporte-forbidden $f-f$ transitions in $\text{Cf}(\text{III})$. The bottom spectrum is that of monoclinic CfBr_3 (the starting material) in the pressure cell at 0.1 GPa. It is identical with the spectrum we reported earlier for this form of CfBr_3 .¹ The middle spectrum, obtained at a pressure of 1.2 GPa, still exhibits most of the features characteristic of monoclinic CfBr_3 but with an increased intensity of the absorption envelope around $13.2 \times 10^5 \text{ m}^{-1}$ relative to that of the peak at $11.4 \times 10^5 \text{ m}^{-1}$. Whether this spectral change reflects the beginning of the transformation from monoclinic CfBr_3 to orthorhombic CfBr_3 or just the effect of pressure on the spectrum of monoclinic CfBr_3 is not known. It should be noted that the top spectrum, obtained at 3.4 GPa, matches the absorption spectrum of orthorhombic CfBr_3 obtained via transmutation of orthorhombic BkBr_3 .¹

Based on our analysis of the absorption spectra obtained from the CfBr_3 sample at several pressures up to 3.4 GPa, we conclude that the structural transformation of monoclinic CfBr_3 to orthorhombic CfBr_3 takes place between 1.7 and 3.4 GPa. As the pressure was further increased up to a maximum of 12.5 GPa and then released in the usual stepwise manner, several reversible spectral features were noted, as well as the irreversibility of the structural transformation. The relative heights of the two peaks at 11.4 and $13.2 \times 10^5 \text{ m}^{-1}$ change with pressure. At higher pressures the peak at $13.2 \times 10^5 \text{ m}^{-1}$ is the more intense; at lower pressures, the $11.4 \times 10^5 \text{ m}^{-1}$ peak is the more intense one. The latter situation describes the absorption spectrum previously identified as that of orthorhombic CfBr_3 .¹ Another reversible spectral change with pressure observed for orthorhombic CfBr_3 was a shift to lower energies with increasing pressure of the cutoff of transmitted light. This shift probably results from the pressure-induced shortening of the ligand-to-metal bond. Such a change decreases the energy of the ligand-to-metal charge-transfer band. A somewhat similar effect was noted recently in a study of the effect of pressure on the spectral and structural properties of AmI_3 .⁶ In the AmI_3 case, however, the shift was further into the visible-wavelength region, occurred at a lower pressure, and was irreversible. It was postulated that this spectral shift may have resulted from the generation of a trace amount of elemental iodine as a consequence of applying pressure on AmI_3 .⁶

As mentioned above, the structural transformation of monoclinic CfBr_3 to orthorhombic CfBr_3 is irreversible with pressure. This transformation may relate to the relative packing efficiencies of the two crystal structures. On the basis of their crystallographic studies of a number of lanthanide trihalides under pressure, Beck and Gladrow proposed the following order of trihalide structures with respect to packing efficiency as pressure is increased: AlCl_3 -type monoclinic (least efficient space filling) < BiI_3 (FeCl_3)-type rhombohedral < UCl_3 -type hexagonal < PuBr_3 -type orthorhombic (most efficient space filling).⁷ The present result is consistent with this sequence. In our previous work we demonstrated the conversion of orthorhombic CfBr_3 to monoclinic CfBr_3 at normal pressure by heating the former to 360 °C.¹ Our direct synthesis of CfBr_3 via hydrobromination of Cf_2O_3 or CfCl_3 always results in monoclinic CfBr_3 . Annealing monoclinic CfBr_3 at various temperatures down to 250 °C does not transform it to the orthorhombic form.

The present result of finding a controllable synthetic route to the orthorhombic form of CfBr_3 opens up the possibility of using applied pressure to produce new modifications of other actinide

(6) Haire, R. G.; Benedict, U.; Young, J. P.; Peterson, J. R.; Begun, G. M. *J. Phys. C*, in press.

(7) Beck, H. P.; Gladrow, E. Z. *Anorg. Allg. Chem.* 1979, 453, 79; 1983, 502, 178.

(5) Mao, H. K.; Bell, P. M.; Shaner, J. W.; Steinberg, D. J. *J. Appl. Phys.* 1976, 49, 3276.

compounds, as well as to produce entirely new compounds such as californium monoxide. Leger and co-workers have already employed pressure-induced reactions to synthesize some lanthanide monoxides.⁸ Further work in our laboratory will explore these possibilities along with increasing our understanding of the effects of pressure, as observed by changes in the optical absorption spectra, on actinide halides.

Acknowledgment. The californium-249 used in this work was made available by the Division of Chemical Sciences, U.S. Department of Energy, through the transplutonium element production facilities at the Oak Ridge National Laboratory. The research was sponsored by the Division of Chemical Sciences, U.S. Department of Energy, partly under contract DE-AS05-76ER04447 with the University of Tennessee, Knoxville (J.R.P.,

J.P.Y., U.B.), and partly under contract DE-AC05-84OR21400 with Martin Marietta Energy Systems, Inc. (R.G.H., G.M.B.).

Registry No. CfBr₃, 20758-68-3.

Department of Chemistry
University of Tennessee
Knoxville, Tennessee 37996-1600

J. R. Peterson^{*9}

Analytical Chemistry and Chemistry Divisions
Transuranium Research Laboratory
Oak Ridge National Laboratory
Oak Ridge, Tennessee 37831

J. P. Young^{10a}
R. G. Haire^{10b}
G. M. Begun^{10b}

Commission of the European Communities
Joint Research Centre
European Institute for Transuranium
Elements
Karlsruhe, Federal Republic of Germany

U. Benedict

- (8) Leger, J. M.; Yacoubi, N.; Loriers, J. "The Rare Earths in Modern Science and Technology"; McCarthy, G. J., Rhyne, J. J., Silber, H. B., Eds.; Plenum Press: New York, 1980; Vol. II, p 203.
(9) Also affiliated with the Chemistry Division, Oak Ridge National Laboratory.
(10) (a) Analytical Chemistry Division. (b) Chemistry Division.

Received March 15, 1985

Articles

Contribution from the Laboratory of Analytical Chemistry, Faculty of Science, Nagoya University, Chikusa, Nagoya 464, Japan, and Faculty of Pharmacy, Meijo University, Tempaku, Nagoya 466, Japan

Equilibria and Kinetics of the Reactions of Water-Soluble Molybdenum(V) Porphyrins with Hydrogen Peroxide in Aqueous Solutions¹

MASAHIKO INAMO,^{2a} SHIGENOBU FUNAHASHI,^{2a} YOSHIO ITO,^{2b} YOSHIKI HAMADA,^{2b} and MOTOHARU TANAKA^{*2a}

Received January 2, 1985

Equilibria of (5,10,15,20-tetrakis(4-*N*-methylpyridiniumyl)porphine(2+))oxomolybdenum(V) (Mo(V)-TMPyP complex) and its reaction with hydrogen peroxide have been investigated in aqueous solutions at $I = 1.00$ M by ESR and visible spectroscopies. The Mo(V)-TMPyP complex hydrolyzes and dimerizes to give rise to the following four species: $[\text{Mo}^{\text{VO}}(\text{tmpyp})\text{OH}]^{4+}$ (1), $[\text{Mo}^{\text{VO}}(\text{tmpyp})\text{OH}]^{4+}$ (2), the bis(μ -hydroxo) dimer $[(\text{tmpyp})\text{OMo}^{\text{VO}}(\mu\text{-OH})_2\text{Mo}^{\text{VO}}(\text{tmpyp})]^{8+}$ (3), and the (μ -hydroxo)(μ -oxo) dimer $[(\text{tmpyp})\text{OMo}^{\text{VO}}(\mu\text{-O})(\mu\text{-OH})\text{Mo}^{\text{VO}}(\text{tmpyp})]^{7+}$ (4). Equilibrium constants were obtained to be $K_{a1} = [2][\text{H}^+][1]^{-1} = 10^{-7.18 \pm 0.02}$ M, $K_{a2} = [4][\text{H}^+][3]^{-1} = 10^{-10.0 \pm 0.1}$ M, and $K_D = [3][2]^{-2} = 10^{6.00 \pm 0.05}$ M⁻¹ at 25 °C. The rate law for the dissociation of dimer 3 to give monomers 1 and 2 is $-d[3]/dt = k_d[3][\text{H}^+]$ with $k_d = (4.1 \pm 0.2) \times 10^4$ M⁻¹ s⁻¹ at 25 °C over the pH range 7.1-7.6. The reaction of the Mo(V)-TMPyP complex with hydrogen peroxide gives three types of peroxo complexes. Over the pH range 5-8 the peroxomolybdenum(V) complex $[\text{Mo}^{\text{VO}}(\text{O}_2)(\text{tmpyp})]^{3+}$ (5) was obtained, while in acidic aqueous solution 1 is oxidized by hydrogen peroxide to produce $[\text{Mo}^{\text{VI}}(\text{O}_2)(\text{tmpyp})\text{OH}]^{6+}$ (6). The substitution of the coordinated water molecule in 6 by hydrogen peroxide yielded a third type of the peroxo complex, $[\text{Mo}^{\text{VI}}(\text{O}_2)_2(\text{tmpyp})]^{4+}$ (7). Formation constants of 5 and 7 were determined to be $K_{\text{Mo(V)}} = [5][\text{H}^+]^2[1]^{-1}[\text{H}_2\text{O}_2]^{-1} = 10^{-9.02 \pm 0.03}$ M and $K_{\text{Mo(VI)}} = [7][\text{H}^+]^2[6]^{-1}[\text{H}_2\text{O}_2]^{-1} = 10^{-8.16 \pm 0.03}$ M, respectively, at 25 °C. The formation of 6 is second order with respect to the concentration of hydrogen peroxide and first order with respect to that of 1, and activation parameters were estimated as follows: $k_{\text{TMPyP}}(25 \text{ }^\circ\text{C}) = 3.27 \times 10^{-4}$ M⁻² s⁻¹, $\Delta H^\ddagger = 74 \pm 1$ kJ mol⁻¹, $\Delta S^\ddagger = -63 \pm 3$ J K⁻¹ mol⁻¹, $\Delta V^\ddagger = 1.3 \pm 0.3$ cm³ mol⁻¹. The mechanism of formation of 5 from 1 and H₂O₂ includes a pre-equilibrium hydrolysis of 1, followed by the rate-determining substitution. Activation parameters for the latter are $k_f(25 \text{ }^\circ\text{C}) = 1.05 \times 10^3$ M⁻¹ s⁻¹, $\Delta H^\ddagger = 37 \pm 1$ kJ mol⁻¹, $\Delta S^\ddagger = -63 \pm 3$ J K⁻¹ mol⁻¹, and $\Delta V^\ddagger = -0.2 \pm 0.3$ cm³ mol⁻¹. An interchange mechanism is most probably operative in this reaction.

Introduction

In recent years the chemistry of molybdenum porphyrins has been extensively investigated. Studies include the synthesis, structural characterization, and chemical reactivities of their dioxygen complexes.³⁻⁶ Complexes of early transition metals in

high oxidation state have been known to react with hydrogen peroxide to produce peroxo complexes. Molybdenum(V) porphyrins give rise to the corresponding peroxomolybdenum(VI) complexes in organic media. Chevrier et al. first reported on the synthesis and crystal structure of diperoxomolybdenum(VI) porphyrin, Mo^{VI}(O₂)₂(tptp).^{3,7} Photochemical⁴ and electro-

- (1) Reactions of Hydrogen Peroxide with Metal Complexes. 8. Preliminary communication: Inamo, M.; Funahashi, S.; Ito, Y.; Hamada, Y.; Tanaka, M. *Chem. Lett.* **1985**, 19. Part 7: Inamo, M.; Funahashi, S.; Tanaka, M. *Inorg. Chem.* **1983**, 22, 3734.
(2) (a) Nagoya University. (b) Meijo University.
(3) Chevrier, B.; Diebold, T.; Weiss, R. *Inorg. Chim. Acta* **1976**, 19, L57.
(4) Ledon, H.; Bonnet, M.; Lallemand, J.-Y. *J. Chem. Soc., Chem. Commun.* **1979**, 702. Ledon, H. J.; Bonnet, M.; Galland, D. *J. Am. Chem. Soc.* **1981**, 103, 6209.

- (5) Kadish, K. M.; Cheng, D.; Malinski, T.; Ledon, H. *Inorg. Chem.* **1983**, 22, 3490.
(6) Imamura, T.; Hasegawa, K.; Fujimoto, M. *Chem. Lett.* **1983**, 705.
(7) Ligand abbreviations: H₂tptp, 5,10,15,20-tetra-*p*-tolylporphine (TpTP); H₂tpp, 5,10,15,20-tetraphenylporphine; H₂tpyp, 5,10,15,20-tetra-4-pyridylporphine (TPyP); H₂tmpyp, 5,10,15,20-tetrakis(4-*N*-methylpyridiniumyl)porphine(4+) (TMPyP); H₂ttmp, 5,10,15,20-tetra-*m*-tolylporphine (TmTP); H₂tpps, 5,10,15,20-tetrakis(4-sulfonatophenyl)porphine (TPPS).